Communication: DFT treatment of strong correlation in 3d transition-metal diatomics

Erin R. Johnson[1, a)] and Axel D. Becke[1, b)]

Department of Chemistry, Dalhousie University, 6274 Coburg Rd, P.O.Box 15000 B3H 4R2, Halifax, Nova Scotia, Canada

(Dated: 21 May 2017)

Bonds between, and to, transition-metal atoms often involve strong electron correlation which cannot be handled by conventional density-functional-theory approximations. The recent "B13" functional of Becke [J. Chem. Phys. 138, 074109 and 161101 (2013)] models dynamic, static, and strong correlation in an exact-exchange-based framework. We test B13 on bond energies of transition-metal diatomics in this work, with promising results.

[a)]Electronic mail: erin.johnson@dal.ca

[b)]Electronic mail: axel.becke@dal.ca

Inclusion of strong correlation is necessary for quantitative prediction of binding energies in transition-metal systems involving multiple metal-metal bonds, such as Cr_2.[1–5] In this molecule, there is formally a hextuple bond between the Cr atoms. One bond involves overlap between the diffuse 4s orbitals, and five involve the more compact 3d orbitals.[1] Since there is little overlap between the 3d orbitals, the situation is similar to stretched H_2,[3,6,7] the prototypical case of strong correlation.[8,9] Although most significant in metal-metal bonds, strong correlation may also stabilize transition-metal oxides and nitrides where there are multiple metal-heteroatom bonds.

Furche and Perdew[2] have compiled a benchmark set of bond energies for diatomic molecules containing 3d transition-metal atoms. The set includes transition-metal hydrides, fluorides, nitrides, oxides, and homonuclear dimers. We expect strong correlation to be important in the latter three classes, thus posing difficult challenges for conventional density-functional theory (DFT) approximations. The hydrides and fluorides, however, involve only single bonds between the heteroatom and the 4s transition-metal orbital, and should be well described by conventional functionals. This is generally the case for organometallic metal-ligand bond energies also.[4,10] Furche and Perdew found[2] that the TPSS[11] "meta-generalised gradient approximation" (meta-GGA) gave the best performance of those tested, yet none provided good across-the-board accuracy.

Wilson *et al.*[5] performed extensive tests of density functionals for bond energies of transition-metal diatomics as well, dividing their benchmark set into systems with either single-reference or multi-reference character. While they ultimately recommended the B97-1 functional,[12,13] they found, like Furche and Perdew, that no functional offered consistently accurate performance, and all gave large errors for Cr_2. Others have used transition-metal bond energies as stringent tests for density-functional theory and wavefunction theory,[14] diffusion quantum Monte-Carlo (DQMC),[15] DFT augmented with a Hubbard-model approach (DFT+U),[16] and the random-phase approximation (RPA).[17,18]

In this work, Furche and Perdew's benchmark set of transition-metal diatomics[2] is used to assess the recent "B13" density functional of Becke[8,9] in particular. This functional explicitly models strong correlation in real space, capturing the spin-restricted dissociation limits of molecular bonds. Furthermore, it is based on 100 percent exactly-computed exchange, thereby obviating the often frustrating task of parametrizing exchange GGAs and meta-GGAs.

The B13 exchange-correlation energy has the form

$$E_{X\text{strong}C}^{\text{B13}} = E_X^{\text{exact}} + E_C^{\text{B13}} + \Delta E_{\text{strong}C}^{\text{B13}}, \tag{1}$$

where E_X^{exact} is the exactly-computed Kohn-Sham (or Hartree-Fock depending on the implementation) exchange energy, E_C^{B13} is the following sum of opposite- and parallel-spin static and dynamic potential energies of correlation:

$$E_C^{\text{B13}} = a_{\text{stat}C}^{\text{opp}} U_{\text{stat}C}^{\text{opp}} + a_{\text{stat}C}^{\text{par}} U_{\text{stat}C}^{\text{par}} + a_{\text{dyn}C}^{\text{opp}} U_{\text{dyn}C}^{\text{opp}} + a_{\text{dyn}C}^{\text{par}} U_{\text{dyn}C}^{\text{par}}, \tag{2}$$

and $\Delta E_{\text{strong}C}^{\text{B13}}$ is a strong-correlation correction given by

$$\Delta E_{\text{strong}C}^{\text{B13}} = \sum_{n=2}^{N} c_n \int x^n u_C d^3\boldsymbol{r}. \tag{3}$$

The four prefactors in Eq. 2 are, to a very good approximation, all equal to each other with optimum value 0.62 (see Ref. 8). Greater accuracy can be achieved, however, by fitting these independently[8,9] with resulting optimum values close to 0.62. In Eq. 3, u_C is the sum of the *integrands* of the four terms in Eq. 2:

$$u_C = u_{\text{stat}C}^{\text{opp}} + u_{\text{stat}C}^{\text{par}} + u_{\text{dyn}C}^{\text{opp}} + u_{\text{dyn}C}^{\text{par}} \tag{4}$$

i.e., the static + dynamic correlation potential-energy density, and x is a dimensionless parameter measuring the relative importance of the static correlation potential-energy density to the total:

$$x = \frac{u_{\text{stat}C}^{\text{opp}} + u_{\text{stat}C}^{\text{par}}}{u_c}. \tag{5}$$

The c_n ($n = 2 \rightarrow N$) are polynomial expansion coefficients fit to strong-correlation test sets.[8,9] Only one or two terms in Eq. 3 are necessary in practice.

We assess the B13 functional with and without the strong correlation correction. Expansion coefficients for the former (the full functional, denoted B13) and the latter (without the strong correlation correction, hereafter denoted B13-0) are as published in Refs. 9 and 8, respectively. All B13 and B13-0 calculations were performed with the grid-based NUMOL program[19] and orbitals from the local-spin-density approximation (LSDA) in the PW91

parameterization;[20] i.e., "post-LSDA". Calculations using the BPBE[21,22] GGA were also performed post-LSDA with NUMOL for direct comparison. The bond lengths were optimized numerically with each of these functionals by varying their values in 0.01 Å increments.

Additional calculations (see Table III) were performed with the Gaussian 09 program[23] using two GGA functionals, BLYP[21,24] and PBE,[22] two meta-GGA functionals, TPSS[11] and M06-L,[25] two hybrid functionals, B3LYP[24,26,27] and PBE0,[28] and two range-separated functionals, LC-ωPBE[29] and HSE06.[30] The 6-311+G(2d,2p) basis set was employed in all cases. In both the NUMOL and Gaussian 09 calculations, atomic d-orbital occupations are as given in Ref. 31. For d^1 configurations, the single electron (or hole) occupies the d_{z^2} orbital. For d^2 configurations, the two electrons occupy the d_{z^2} and $d_{x^2-y^2}$ orbitals, which are the "e" orbitals in octahedral symmetry.

First, the performance of B13 and B13-0 is assessed on s-d transfer energies of the free transition-metal atoms. These are excitation energies for the atomic transitions $d^m s^n \rightarrow d^{m+1} s^{n-1}$. As shown by Furche and Perdew,[2] accurate prediction of s-d transfer energies is particularly challenging for DFT approximations due to the significant difference in exchange-correlation energies between the ground-state and excited-state configurations. Table I lists B13, B13-0, and BPBE GGA s-d transfer energies. Like other GGAs, BPBE severely underestimates s-d transfer energies,[2] even predicting the incorrect ground state for Ti, V, Fe, and Co. Furche and Perdew found that inclusion of some exact exchange improves the results. In particular, B3LYP gave the lowest MAE (mean absolute error) of the functionals considered in that work (0.36 eV) and recovers the correct ground state for Ti. B3LYP still incorrectly favours the s^1 configuration for V, Fe, and Co however.[2] In the present work, we also find that the exact-exchange-based functionals give improved results, with B13 providing the lowest MAE of 0.35 eV. Both B13 and B13-0 recover the correct ground states for Ti and Fe, but only B13 predicts the correct ground state for Co. Otherwise there is very little difference between the two B13 variants. This is as expected, since there is minimal strong electron correlation in isolated atoms having a single-determinant reference configuration.

Bond energies for the full set of 3d transition-metal diatomics are given in Table II for the BPBE, B13-0, and B13 functionals. The lowest-energy configuration of each free transition-metal atom, obtained with each functional as in Table I, was used in evaluating the bond energies. The experimental ground-state multiplicity, as reported in the work of Furche

TABLE I: Calculated s-d transfer energies, in eV, for the 3d transition-metal atoms. All calculations were performed using the NUMOL program. Experimental data taken from Reference 2 is included for comparison. The mean absolute error (MAE), mean error (ME), and maximum error (MaxE) are given for each functional.

Atom	Excitation	BPBE	B13-0	B13	Expt.
Ca	$d^0s^2 \rightarrow d^1s^1$	1.40	2.03	1.88	2.44
Sc	$d^1s^2 \rightarrow d^2s^1$	0.22	0.85	0.71	1.33
Ti	$d^2s^2 \rightarrow d^3s^1$	-0.46	0.27	0.11	0.69
V	$d^3s^2 \rightarrow d^4s^1$	-1.03	-0.26	-0.42	0.11
Cr	$d^4s^2 \rightarrow d^5s^1$	-2.24	-1.47	-1.64	-1.17
Mn	$d^5s^2 \rightarrow d^6s^1$	0.69	1.25	1.52	1.97
Fe	$d^6s^2 \rightarrow d^7s^1$	-0.37	0.11	0.43	0.65
Co	$d^7s^2 \rightarrow d^8s^1$	-0.70	-0.27	0.14	0.17
Ni	$d^8s^2 \rightarrow d^9s^1$	-0.99	-0.66	-0.25	-0.33
Ni	$d^9s^1 \rightarrow d^{10}s^0$	1.41	1.36	1.64	1.57
Cu	$d^9s^2 \rightarrow d^{10}s^0$	-2.28	-1.95	-1.64	-1.85
	MAE	0.90	0.39	0.35	–
	ME	-0.90	-0.39	-0.28	–
	MaxE	-1.28	-0.72	-0.62	–

and Perdew,[2] was assumed for each molecule. All calculations on singlet species were spin-restricted. The results in Table II show that BPBE strongly over-binds the majority of these diatomics, the largest errors occurring for the oxides (particularly MnO and FeO) and for Ni_2^+. The last result is understandable, since Ni_2^+ involves a positive charge delocalized over both atoms, and will hence be overly stabilized by local functionals such as the LSDA and GGAs.[7,32–35] This is analogous to the well-known H_2^+ dissociation-curve disaster.[6,7] Conversely, B13-0 tends to under-bind the nitrides and oxides, and severely under-binds many of the homonuclear dimers (V_2^+ and V_2). Some are not even bound (Cr_2, Fe_2, Co_2, and Ni_2).

All the failures of B13-0 occur for multiple bonds involving both s and d orbitals of the transition-metal atoms, the cases where strong correlation plays a role. Thus B13, which explicitly models strong correlation, gives the lowest MAE of the three functionals in Table II, with no systematic over-binding or under-binding tendency. Figure 1 illustrates the behaviour of B13 and B13-0 for the different classes of diatomics, showing MAE and ME (mean error) values for the transition-metal hydrides, fluorides, oxides, nitrides, and homonuclear dimers. Both functionals perform similarly for the hydrides and fluorides where there is only a single bond to the diffuse s orbital of the metal atom. Where strong correlation is important, however, in the oxides, nitrides, and especially the homonuclear dimers, B13-0

TABLE II: Computed binding energies, in kcal/mol, for the complete set of 3d transition-metal diatomics. All calculations were performed using the NUMOL program. Experimental data obtained from Reference 2 is included for comparison. The mean absolute error (MAE) and mean error (ME) are given for each functional.

Diatomic	BPBE	B13-0	B13	Expt.
KH	40.9	41.6	44.3	42.2
CaH	47.7	39.9	41.0	41.0
ScH	56.0	56.9	57.9	47.5
TiH	57.2	52.7	57.9	50.0
VH	56.7	56.9	58.3	51.4
CrH	50.3	48.5	48.8	46.8
MnH	47.9	41.4	37.5	31.1
FeH	53.5	46.9	37.5	39.2
CoH	59.8	56.4	52.1	48.4
NiH	65.2	65.2	67.3	61.3
CuH	63.8	67.2	66.0	63.4
KF	120.1	120.4	119.7	117.5
CaF	138.9	132.2	132.9	127.2
ScF	148.3	146.4	147.7	143.3
TiF	143.3	133.5	139.1	137.0
CrF	115.6	112.7	110.8	106.3
CuF	98.7	102.0	96.3	102.8
ScN	120.1	93.7	100.8	113.0
TiN	132.7	116.2	127.4	124.0
VN	124.9	108.0	117.3	117.0
CrN	99.9	73.2	82.8	97.0
CaO	124.2	102.8	110.6	110.8
ScO	181.7	161.6	171.1	163.0
TiO	177.0	158.8	171.2	161.0
VO	162.8	142.2	153.0	150.0
CrO	115.8	95.2	101.6	103.0
MnO	126.9	92.1	93.8	89.5
FeO	127.9	96.2	99.1	97.4
CoO	110.4	70.5	87.6	92.1
NiO	109.0	59.2	82.4	90.4
CuO	74.4	51.4	57.8	66.6
K_2	9.5	11.7	14.2	12.0
Ti_2	59.8	23.4	56.1	36.1
V_2^+	85.4	40.0	86.5	73.2
V_2	66.9	30.3	71.6	64.3
Cr_2	20.0	-10.1	55.0	33.9
Fe_2	58.2	-18.7	10.4	26.9
Co_2	54.3	-43.5	21.0	39.4
Ni_2^+	101.3	45.1	66.5	52.2
Ni_2	57.0	-10.1	33.5	48.1
Cu_2	46.5	52.7	47.3	46.7
MAE	12.0	13.6	6.9	–
ME	10.9	-9.8	1.7	–

FIG. 1: Mean absolute errors (solid lines) and mean errors (dashed lines) in the computed B13-0 and B13 bond energies for each sub-class of the 3d transition-metal diatomic set.

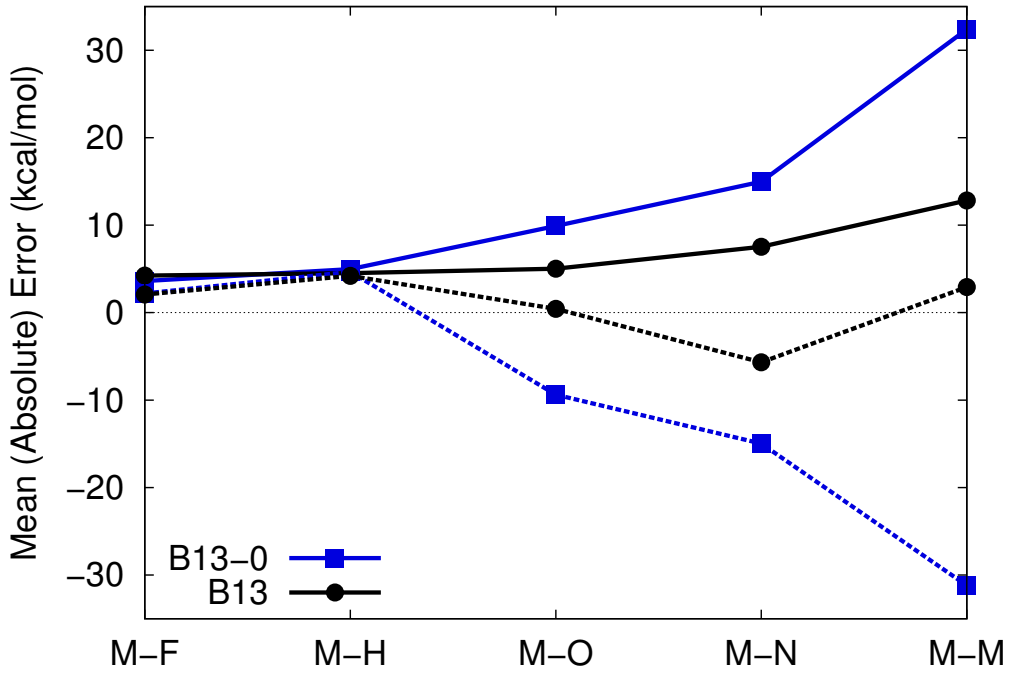

clearly under-binds. The strong-correlation term in B13 nicely corrects this error.

To place the performance of B13 in a wider context, we compare with some popular GGA, hybrid, and range-separated hybrid functionals in Table III. This is not an exhaustive survey, rather a reflection of the effect of differing degrees of exact-exchange mixing on the bond energies. More extensive tests can be found in the papers of Wilson *et al.*[5] and of Truhlar *et al.*[14] Table III reveals that all of the functionals involving exact exchange, excepting B13, give large MAEs and systematically under-estimate the bond energies. GGAs and meta-GGAs (without exact exchange) also give large MAEs, but with an over-binding tendency. M06-L is the best performing of these, but note that 3d transition-metal diatomics, including Cr_2, are part of the extensive parametrization set used in its fitting.[25] For most of the considered functionals, the greatest over-binding occurs in Ni_2^+ due to the large delocalization error mentioned earlier. The effect of this error is largest for the GGAs and meta-GGAs, but is reduced through exact-exchange mixing in the hybrids and range-separated hybrids. B13-0 and B13 both use 100 percent exact exchange and exhibit the lowest Ni_2^+ errors.

Cr_2 is typically the most problematic under-bound system, due to neglect of strong correlation in conventional functionals. All functionals that under-bind Cr_2 also greatly underestimate its bond length. The errors are largest for the hybrid and range-separated hybrid

TABLE III: Bond-energy error statistics for the complete set of 3d transition-metal diatomics obtained with selected density functionals. Max+ indicates the maximum positive error (over-binding) and Max− indicates the maximum negative error (under-binding). All quantities are in kcal/mol. The B13-0 and B13 calculations were performed with NUMOL. All other calculations were performed with Gaussian 09 using the 6-311+G(2d,2p) basis set.

Method	MAE	ME	Max +		Max −	
B13-0	13.6	-9.8	10.3	MnH	-82.9	Co_2
PBE0	13.5	-9.2	21.2	Ni_2^+	-111.6	Cr_2
HSE06	13.1	-8.8	21.4	Ni_2^+	-108.7	Cr_2
LC-ωPBE	14.8	-5.8	21.8	Ni_2^+	-113.1	Cr_2
B3LYP	10.4	-4.4	26.1	Ni_2^+	-74.4	Cr_2
B13	6.9	1.7	21.1	Cr_2	-18.4	Co_2
M06-L	8.1	5.3	44.9	Ni_2^+	-30.9	Cr_2
TPSS	11.3	10.3	48.0	Ni_2^+	-16.5	Cr_2
BLYP	13.0	12.8	49.3	Ni_2^+	-4.2	CuF
PBE	14.3	13.8	53.0	Ni_2^+	-7.3	Cr_2

TABLE IV: Bond-energy error statistics for the subset of homometallic diatomics obtained with selected density functionals using either spin-symmetic or broken-symmetry calculations. Max− indicates the maximum negative error (under-binding). All quantities are in kcal/mol. The B13-0 and B13 calculations were performed with NUMOL. All other calculations were performed with Gaussian 09 using the 6-311+G(2d,2p) basis set.

Method	Spin-symmetric				Broken-symmetry			
	MAE	ME	Max −		MAE	ME	Max −	
B13-0	32.4	-31.2	-82.9	Co_2	–	–	–	–
LC-ωPBE	33.5	-29.2	-113.1	Cr_2	19.6	-14.0	-62.8	V_2
PBE0	32.2	-28.1	-111.6	Cr_2	17.6	-13.4	-55.6	V_2
HSE06	30.5	-26.2	-108.7	Cr_2	16.9	-12.6	-53.0	V_2
B3LYP	22.7	-17.5	-74.4	Cr_2	13.0	-7.7	-37.7	V_2
B13	12.8	2.9	-18.4	Co_2	–	–	–	–
M06-L	14.1	6.2	-30.9	Cr_2	12.1	10.3	-5.9	V_2^+
TPSS	14.4	11.1	-16.5	Cr_2	13.2	12.5	-3.6	Cr_2
BLYP	17.5	17.5	0.0	Cu_2	18.1	18.1	0.0	Cu_2
PBE	19.1	17.6	-7.3	Cr_2	18.5	18.4	-0.4	Cr_2

functionals, up to 0.158 Å with LC-ωPBE. B13, on the other hand, gives a reasonably accurate bond length of 1.65 Å compared to the experimental value of 1.68 Å.

In the past, many computations on homometallic diatomics have used broken spin symmetry to simulate strong correlation (i.e. localization of excess α-spin density on one nucleus

and excess β-spin density on the other). The effect of symmetry breaking on the homometallic bond energies is shown in Table IV. Among the systems studied here, symmetry breaking gives lower energies for Cr_2 and Ni_2 with all functionals, and also for Fe_2, V_2, and V_2^+ for those functionals with exact-exchange mixing. A variational broken-symmetry analysis is not possible for the B13 and B13-0 functionals because of their non-self-consistent implementation. Note, however, that B13 is fundamentally designed not to favor spin polarization. The results in Table IV reveal that symmetry breaking significantly reduces the extent of under-binding in hybrid functionals, particularly for Cr_2, but a systematic under-binding tendency still remains.

Overall, B13 substantially outperforms all the other functionals in Table III, having the lowest MAE. Moreover, its ME is nearest to zero, indicating that it neither systematically over-binds or under-binds. Self-consistent (SC) implementation of B13 is highly challenging, as it requires not only the local density, the gradient and Laplacian of the density, and the kinetic-energy density, but the exact local exchange-energy density as well.[8,9] Despite these complications, SC implementation of an earlier and related functional, "B05",[36] has been accomplished.[37] We therefore hope the present results will encourage ongoing development of B05 and B13 technology.

Acknowledgements: The authors thank the Natural Sciences and Engineering Research Council of Canada (NSERC) for financial support and the Atlantic Computational Excellence network (ACEnet) for computational resources.

REFERENCES

[1]K. E. Edgecombe and A. D. Becke, Chem. Phys. Lett. **244**, 427 (1995).

[2]J. P. Perdew and F. Furche, J. Chem. Phys. **124**, 044103 (2006).

[3]A. J. Cohen, P. Mori-Sánchez, and W. Yang, J. Chem. Phys. **129**, 121104 (2008).

[4]E. R. Johnson and A. D. Becke, Can. J. Chem. **87**, 1369 (2009).

[5]W. Jiang, M. L. Laury, M. Powell, and A. K. Wilson, J. Chem. Theory Comput. **8**, 4102 (2012).

[6]A. D. Becke, J. Chem. Phys. **119**, 2972 (2003).

[7]A. J. Cohen, P. Mori-Sánchez, and W. Yang, Science **321**, 792 (2008).

[8]A. D. Becke, J. Chem. Phys. **138**, 074109 (2013).

[9]A. D. Becke, J. Chem. Phys. **138**, 161101 (2013).

[10]C. A. Jiménez-Hoyos, B. G. Janesko, and G. E. Scuseria, J. Phys. Chem. A **113**, 11742 (2009).

[11]J. Tao, J. P. Perdew, V. N. Staroverov, and G. E. Scuseria, Phys. Rev. Lett. **91**, 146401 (2003).

[12]A. D. Becke, J. Chem. Phys **107**, 8554 (1997).

[13]F. Hamprecht, A. Cohen, D. Tozer, and N. Handy, J. Chem. Phys. **109**, 6264 (1998).

[14]X. Xu, W. Zhang, M. Tang, and D. G. Truhlar, J. Chem. Theory Comput. **11**, 2036 (2015).

[15]K. Doblhoff-Dier, J. Meyer, P. E. Hoggan, G.-J. Kroes, and L. K. Wagner, J. Chem. Theory Comput. **12**, 2583 (2016).

[16]H. J. Kulik and N. Marzari, J. Chem. Phys. **133**, 114103 (2010).

[17]J. E. Bates, P. D. Mezei, G. I. Csonka, J. Sun, and A. Ruzsinszky, J. Chem. Theory Comput. **13**, 100 (2017).

[18]C. Waitt, N. M. Ferrara, and H. Eshuis, J. Chem. Theory Comput. **12**, 5350 (2016).

[19]A. D. Becke and R. M. Dickson, J. Chem. Phys. **92**, 3610 (1990).

[20]J. P. Perdew and Y. Wang, Phys. Rev. B **45**, 13244 (1992).

[21]A. D. Becke, Phys. Rev. A **38**, 3098 (1988).

[22]J. Perdew, K. Burke, and M. Ernzerhof, Phys. Rev. Lett. **77**, 3865 (1996).

[23]M. J. Frisch, G. W. Trucks, H. B. Schlegel, G. E. Scuseria, M. A. Robb, J. R. Cheeseman, G. Scalmani, V. Barone, B. Mennucci, G. A. Petersson, H. Nakatsuji, M. Caricato, X. Li, H. P. Hratchian, A. F. Izmaylov, J. Bloino, G. Zheng, J. L. Sonnenberg, M. Hada, M. Ehara, K. Toyota, R. Fukuda, J. Hasegawa, M. Ishida, T. Nakajima, Y. Honda, O. Kitao, H. Nakai, T. Vreven, J. A. Montgomery, Jr., J. E. Peralta, F. Ogliaro, M. Bearpark, J. J. Heyd, E. Brothers, K. N. Kudin, V. N. Staroverov, R. Kobayashi, J. Normand, K. Raghavachari, A. Rendell, J. C. Burant, S. S. Iyengar, J. Tomasi, M. Cossi, N. Rega, J. M. Millam, M. Klene, J. E. Knox, J. B. Cross, V. Bakken, C. Adamo, J. Jaramillo, R. Gomperts, R. E. Stratmann, O. Yazyev, A. J. Austin, R. Cammi, C. Pomelli, J. W. Ochterski, R. L. Martin, K. Morokuma, V. G. Zakrzewski, G. A. Voth, P. Salvador, J. J. Dannenberg, S. Dapprich, A. D. Daniels, . Farkas, J. B. Foresman, J. V. Ortiz, J. Cioslowski, and D. J. Fox, "Gaussian 09 Revision A.1," Gaussian Inc. Wallingford CT

2009.

[24]C. Lee, W. Yang, and R. G. Parr, Phys. Rev. B **37**, 785 (1988).

[25]Y. Zhao and D. G. Truhlar, J. Chem. Phys. **125**, 194101 (2006).

[26]A. D. Becke, J. Chem. Phys. **98**, 5648 (1993).

[27]P. J. Stephens, F. J. Devlin, C. F. Chabalowski, and M. J. Frisch, J. Phys. Chem. **98**, 11623 (1994).

[28]C. Adamo and V. Barone, J. Chem. Phys. **110**, 6158 (1999).

[29]O. A. Vydrov and G. E. Scuseria, J. Chem. Phys. **125**, 234109 (2006).

[30]A. V. Krukau, O. A. Vydrov, A. F. Izmaylov, and G. E. Scuseria, J. Chem. Phys. **125**, 224106 (2006).

[31]E. R. Johnson, R. M. Dickson, and A. D. Becke, J. Chem. Phys. **126**, 184104 (2007).

[32]Y. K. Zhang and W. T. Yang, J. Chem. Phys. **109**, 2604 (1998).

[33]A. Ruzsinszky, J. P. Perdew, G. I. Csonka, O. A. Vydrov, and G. E. Scuseria, J. Chem. Phys. **125**, 194112 (2006).

[34]M.-C. Kim, E. Sim, and K. Burke, Phys. Rev. Lett. **111**, 073003 (2013).

[35]E. R. Johnson, A. Otero-de-la Roza, and S. G. Dale, J. Chem. Phys. **139**, 184116 (2013).

[36]A. D. Becke, J. Chem. Phys. **122**, 064101 (2005).

[37]E. Proynov, F. Liu, Y. Shao, and J. Kong, J. Chem. Phys. **136**, 034102 (2012).